UNIVERSITY
OF GÄVLE

ITB/Electronics

Dynamic nonlinear pre-distortion of signal generators for improved dynamic range

Suzan Jawdat

June 2009

Master's Thesis in Electronics/Telecommunication
Supervisor : Dr. Niclas Björsell
Examiner : Dr. Magnus Isaksson

Abstract

In this thesis, a parsimoniously parameterized digital predistorter is derived for linearization of the IQ modulation mismatch and the amplifier imperfection in the signal generator [1]. It is shown that the resulting predistorter is linear in its parameters, and thus they may be estimated by the method of least-squares. Spectrally pure signals are an indispensable requirement when the signal generator is to be used as part of a test bed. Due to the non-linear characteristic of the IQ modulator and power amplifier, distortion will be present at the output of the signal generator. The device under test was the IQ modulation mismatch and power amplifier deficiencies in the signal generator.

In [2], the dynamic range of low-cost signal generators are improved by employing model based digital pre-distortion and the designed predistorter seems to give some improvement of the dynamic range of the signal generator.

The goal of this project is to implement and verify the theory parts [1] using data program (Matlab) to improve the dynamic range of the signal generator. The design digital pre-distortion that is implemented in software so that the dynamic range of the signal generator output after predistortion is superior to that of the output prior to it. In this project, we have observed numerical problems in the proposed theory and we have found other methods to solve the problem.

The polynomial model is commonly used in power amplifier modeling and predistorter design. However, the conventional polynomial model exhibits numerical instabilities when higher order terms are included, we have used the conventional and orthogonal polynomial models. The result shows that the orthogonal polynomial model generally yield better power amplifier modeling accuracy as well as predistortion linearization performance then the conventional polynomial model.

Acknowledgements

Firstly, I would like to give my deep and sincere gratitude to my supervisor, Dr. Niclas Björsell, for giving me the opportunity to perform this thesis and helping me during my work.

I would like to thanks Prof. Peter Händel for his wonderful project description.

I also would like to thanks, Charles Nader, Per Landin and Carl Karlsson for helping me in my project.

Finally, I would like to gratitude my family they had always helped and supported me during my live and the academy.

Contents

1 Introduction 1

1.1 Background 1

1.2 Objective 3

1.3 Thesis outline 3

2 Theory 4

2.1 Introduction 4

2.2 Linear systems 6

2.2.1 Predistortion 6

2.2.2 Analog predistortion 7

2.2.3 Digital predistortion 8

2.3 The baseband equivalent 8

2.4 Predistorter design based on physical modelling 10

2.4.1 IQ imbalance 12

2.4.2 Predistortion mirror distortion 14

2.4.3 Power amplifier deficiencies 16

2.5 Parsimonious predistorter structures 18

2.5.1 Linear part of the predistorter 19

2.5.2 Non linear part of the predistorter 21

2.6 Predistorter properties 22

2.7 Training of the predistorter based on N-sequences of data 24

2.7.1 Model output 24

2.7.2 Least-squares problem 27

2.7.3 Determination of the function $\beta(\cdot)$ 28

3 Method 29

3.1 Introduction 29

3.2 Test setup 29

3.2.1 The implemented system 29

3.2.2 Vector Signal Generator 31

3.2.3 Vector Signal Analyzer 32
3.3 Simulation model 33
3.4 Determinate parameters 34
3.4.1 Gamma (γ) 34
3.4.2 Model order $(M \ \& \ L)$ 34
3.4.3 Basis function $\psi_m(\cdot)$ or $\phi_m(\cdot)$ 35
3.4.4 Realization 35
4 Results 36
4.1 Introduction 36
4.2 Simulation results 36
4.3 Measurement results 43
5 Discussion 48
6 Conclusions 49
7 References 50

List of Figures

Figure 1.1. The implemented system 2

Figure 2.1. IQ signal transmission 5

Figure 2.2. Predistortion main ideas 7

Figure 2.3. Baseband equivalent 9

Figure 2.4. Digital predistortion design 11

Figure 2.5. IQ imperfection in the signal generator 12

Figure 2.6. Digital predistortion design for IQ imbalance 13

Figure 2.7. Training of the digital predistorter $F(s_n;\theta)$. 15

Figure 2.8. Digital predistortion design for power amplifier 16

Figure 2.9. Digital predistorter where input signal x_n produces output signal z_n 21

Figure 3.1. Calibration set-up 30

Figure 3.2. Hardware from IF to the process 32

Figure 3.3. Gamma (γ) 34

Figure 4.1. Power spectrum of two-tone signal without predistortion 37

Figure 4.2. Power spectrum of two-tone signal with predistortion 38

Figure 4.3. Power spectrum of two-tone signal $\phi_m(\cdot)$ function without predistortion .. 39

Figure 4.4. Power spectrum of two-tone signal $\phi_m(\cdot)$ function with predistortion 40

Figure 4.5. Power spectrum of two-tone signal $\psi_m(\cdot)$ function without predistortion .. 41

Figure 4.6. Power spectrum of two-tone signal $\psi_m(\cdot)$ function with predistortion 42

Figure 4.7. Power spectrum of two-tone signal $\phi_m(\cdot)$ function without predistortion .. 44

Figure 4.8. Power spectrum of two-tone signal $\phi_m(\cdot)$ function with predistortion 45

Figure 4.9. Power spectrum of two-tone signal $\psi_m(\cdot)$ function without predistortion ... 46

Figure 4.10. Power spectrum of two-tone signal $\psi_m(\cdot)$ function with predistortion 47

Abbreviations

ADC	Analog to digital converter
AWG	Arbitrary waveform generator
ATT	Attenuation
DAC	Digital analog conversion
DUT	Device under test
FT	Fourier transfer
IF	Intermediate frequency
IQ	In-phase Quadrature phase
LAN	Local area network
LO	Local oscillator
LUT	Look up table
NCO	Numerical controlled oscillator
PA	Power amplifier
PC	Personal computer
PD	Pre-distortion
RBW	Resolution bandwidth
REF	Reference level
RF	Radio frequency
SA	Signal analyzer
SG	Signal generator
VBW	Video bandwidth

1 Introduction

1.1 Background

When measuring the performance of high-quality components, such as analog to digital converters (ADC) and power amplifiers (PA), one must ensure that the test setup has superior performance compared to the device under test (DUT). In some test setups the signal generator (SG) is the weak link. Even state-of-the-art signal generators can have problem to generate spectrally pure enough signals for some applications. Nonlinearities and other imperfection in the generator results in problems with harmonic distortion and intermodulation products in the generated signal. Today, most of the electrical signals are processed in the digital system performance, and as a result of the ADC present on the border to the digital domain [3].

The evolution of digital signal processing enables cost-efficient trade-offs between performance boosting by digital operations and cost-reduction by reduction the requirements on the analog hardware. Even though the SG hardware is insufficient, spectrally pure signals can be generated by using software. A modern SG is equipped with an arbitrary waveform generator (AWG), where the waveform is a time series created in a computer program for example (Matlab). A method is to generate the wanted signal and measure the actually generated signal. Thereafter calculate a pre-distorted (PD) signal that is adjusted to compensate for the distortion. The device under test was the IQ modulation mismatch and the amplifier imperfection in the signal generator. We consider digital pre-distortion of radio frequency signal generators by means of parametric dynamic modelling of the inverse of the nonlinear artifacts, in order to improve the dynamic range of the analyzer.

The aim of this project is to implement and verify the theory parts using data program (Matlab) in software to give some improvement of the dynamic range of the signal generator. The signal is measured by a signal analyzer (SA) that is connected to a person

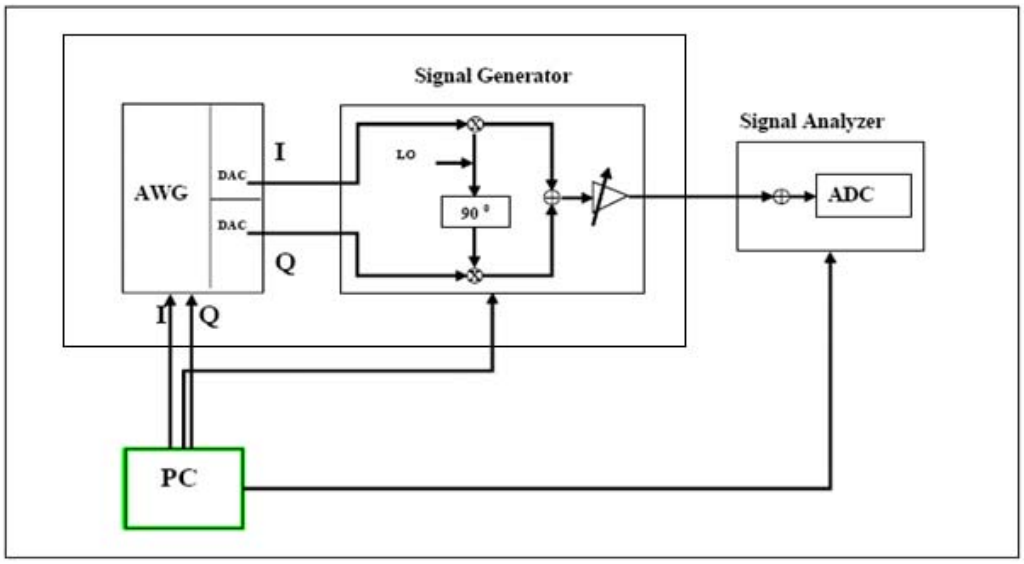

Figure 1.1. The implemented system

computer (PC) via a local area network (LAN) as shown in Figure 1.1. The same PC is used to generate time series to the SG (that also is connected to the LAN).

A parsimoniously parameterized digital pre-distorter is derived starting with 'grey box' models of the IQ modulation mismatch and the amplifier imperfections. The pre-distorter may be estimated by the method of least-squares. The resulting pre-distortion algorithm – containing of linear time invariant filters, summations and multiplications, only – is expected to handle frequency varying IQ modulation mismatch and amplifier deficiencies with memory [1].

1.2 Objective

In this project, we will implement an automatic method for generating spectrally pure signals using digital pre-distortion design. This works includes theory parts from [1], my task is to implement and verify the theory parts using data program (Matlab) in software to give some improvement of the dynamic range of the signal generator, under an assumption that the distortion produced by the signal generator dominates the distortion by the instruments in the set-up.

1.3 Thesis Outline

The first Chapter of this thesis is introduction that provides general information about the content of the thesis. It intends to set the introduction, background and the objective of this project. The second Chapter includes all the theoretical and mathematical information required to understand the work. The third Chapter contains the technical and theoretical information that was used to have the appropriate test setup, simulation and measurement procedure along the whole thesis. Chapter fourth includes the simulation and measurement results. Chapter fifth presents the analyze and discussion of the results.

2 Theory

2.1 Introduction

In-phase quadrature (IQ) signal processing is a widely used tool in modulated systems and radio communications in order to take full advantage of the available resources (such as the transmission bandwidth). In communications signal processing, it is common to use the notation of complex-valued signal. As an illustration, two oscillator signals with a 90º phase difference, $\cos(2\pi f_0 t)$ and $\sin(2\pi f_0 t)$, can be conveniently modelled as a complex oscillator $\cos(2\pi f_0 t) + j\sin(2\pi f_0 t) = e^{j2\pi f_0 t}$. In practice, a complex-valued signal is simply a pair of two real-valued signals carrying the real and imaginary parts.

The benefit of employing and processing complex-valued signals is most conveniently described in frequency domain. For a real-valued signal, say $x(t)$, the Fourier transform (FT) $X(f)$ obeys the Hermitian symmetry, i.e., $X(-f) = X^*(f)$ where the superscript $(\cdot)^*$ denotes complex conjugation [4]. In radio communications, the concept of complex-valued or IQ signals was initially enabled and justified by the virtue of bandpass signal transmission. In general, using the lowpass–to-bandpass transformation, a complex-valued baseband signal $z(t) = z_I(t) + z_Q(t)$ can be transmitted in a real-valued channel.

$$U(t) = \mathrm{Re}\left[z(t)e^{jwt}\right] = z_I(t)\cos(wt) - z_Q(t)\sin(wt)$$

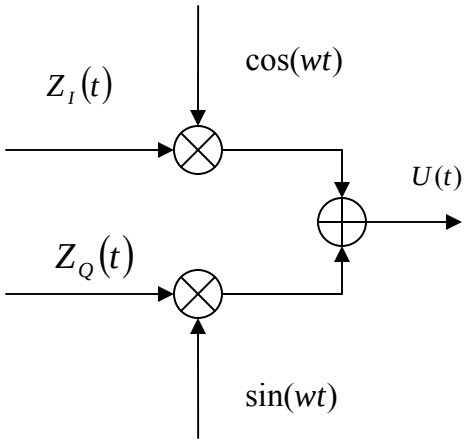

Figure 2.1. IQ signal transmission

where w denotes the carrier angular frequency in rad /s and Re[x] refers to the real part of a complex-valued quantity x, according to Figure 2.1 two real-valued messages $z_I(t)$ and $z_Q(t)$ can be transmitted over the same bandwidth resulting in increased spectral efficiency. The IQ signal processing has the ability to process the negative and positive frequencies separately is strictly valid only if the I and Q branches are perfectly matched but some unintentional variations between the amplitudes and phases of such a two-branch structure will always take place. The I and Q branch mixers are two separate physical components, their characteristics always differ from one another to some extent. The two local oscillator (LO) signals should ideally have equal amplitudes and an exact phase difference of 90º [4]. In practice, there exists a small non-90° phase error between the I and Q channels of an IQ modulator. Also, the I and Q channels may not always have the same amplitude. The phase error and amplitude imbalance cause unwanted image signals that are generated in-band and consequently, degrades the system performance [5]. Within this project digital pre-distortion will be designed to increase the system performance and minimize the phase error and amplitude imbalance in the IQ channel.

The radio frequency (RF) power amplifier (PA) is a key component in modern telecommunication systems since its power consumption dominates the other parts in the system. The purpose of the RF PA is to amplify the radio signal to a necessary power level for transmission to the receiver. RF PAs are divided into different classes, i.e. A, AB, B etc. with respect to their power efficiency. In RF PAs there is a trade-off between efficiency and linearity. High efficiency and high linearity cannot be achieved at the same time [6]. In the case of amplifier for the transmitter so the efficiency is an important parameter of an amplifier; however, to obtain the maximum efficiency the amplifier is usually pushed into non-linear region. This in turn induces intermodulation products. The non linear region is the region where the gain of the amplifier does not increase linearly with the increment of the input. One of the most promising applications of dynamic behavioural modelling of RF PAs is digital predistortion. The digital predistortion is achieved by designing the predistorter to be as close as possible to the inverse of the power amplifier function to get a desired output signal from the signal generator.

2.2 Linear systems

Linear system is a mathematical model of a system based on the use of a linear operator. As a mathematical abstraction or idealization, linear systems find important applications in automatic control theory, signal processing, and telecommunications. Linearization is used to make (nonlinear) systems behave more linear. This means less spectral distortion. Predistortion is one of the most promising linearization techniques

2.2.1 Predistortion

Predistortion is a technique consisting of introducing the inverse of the unwanted characteristic of the DUT of the power amplifier, in series with the DUT, to eliminate the distortion introduced by the unwanted DUT's characteristic [7].

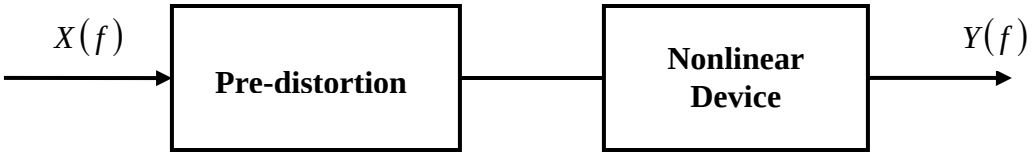

Figure 2.2. Predistortion main ideas

In this work, the predistortion design used to improve the dynamic range of the IQ modulation and power amplifier of the signal generators. It is a cost-saving technology and it can be done in an analog as well as digital manner. Pre-distortion is an application of behavioural modelling in which the input signal is predistorted -or precorrected- in order to achieve a desired output signal. An ideal predistorter is the inverse of the system's response function. The predistorted input signal is calculated from the desired output signal by the predistorter [8]. The goal of the predistortion system is to make the cascade of the predistorter for IQ modulation and power amplifier. This is achieved by designing the PD to be as close as possible to the inverse of the IQ modulation and power amplifier function.

2.2.2 Analog predistortion

The advantages of analog predistortion are relatively simple low-cost, low energy consumption, wideband signal handling capability and integrity. If they are implemented adaptively, then the system complexity may increase significantly. There are different ways to implement the analog predistortion. It can be a simple circuit composed of diodes or transistors as in RF predistorters, or it can be composed of multipliers to realize polynomial nonlinearities [9]. The system can be adaptive or fixed depending on environmental conditions and system specifications. However, a reliable system must have a kind of adaptation adjusting the predistorter according to the environmental conditions especially in today's mobile communication systems, which may operate

under extreme conditions and still must fulfil the specifications. High linearity system based on RF predistortion is extremely difficult to achieve and are not widely available. There are three analogue linearization techniques; power back-off, feed forward linearization techniques, and Cartesian-loop linearization, details are given in [10].

2.2.3 Digital predistortion

Digital predistortion is usually implemented in digital baseband but it is also possible to do it at intermediate frequency (IF). The theory behind is the same as in analog predistortion. This method is in general used for base stations in mobile communication systems in order to improve linearity, which is very important in systems with wide bandwidths. A significant improvement can be achieved for class B and AB in applications requiring high linearity. Digital predistortion is simple compared to feed forward linearization widely used in base stations. It is unconditionally stable and a precise linearization is possible [9].

There are two digital linearization techniques; Look up table (LUT) and polynomial pre-distorter. Look up table based predistorter stores the pre-distortion coefficients for all input values in the LUT and the incoming signal is multiplied sample with this coefficient. In the polynomial pre-distorter case, the characteristics of the signal generator and the pre-distorter are described by polynomial functions. The polynomial coefficients of the pre-distorter are adjusted to compensate the DUT nonlinearity, resulting in a linear system [7].

2.3 The baseband equivalent

In signal processing, baseband is an adjective that describes signals and systems whose range of frequencies is measured from zero to a maximum bandwidth or highest signal frequency. The physical signal corresponds to $z_I(t)\cos(wt) - z_Q(t)\sin(wt) = \mathrm{Re}\{z(t)e^{jwt}\}$ where ω is the carrier angular frequency in rad /s.

Power amplifier is a device that changes, usually increases, the amplitude of a signal. The signal is usually voltage or current. The relationship of the input to the output of an amplifier usually expressed as a function of the input frequency is called the transfer function of the amplifier, and the magnitude of the transfer function is termed the gain.

In this work, the baseband equivalent is given in Figure 2.3, the signal generator equipment chain is modelled by the nonlinear dynamic function $G(\cdot)$ and $H(\cdot)$, respectively. $G(\cdot)$ and $H(\cdot)$ describing the IQ and power amplifier deficiencies are unknown and have to be estimated. The signal u_n is a baseband representation of the IQ modulator output prior to the power amplification. The predistorter transforming the reference stimuli r_n into the signal generator input z_n is denoted by $F(\cdot)$. The aim of the predistorter $F(\cdot)$ is to minimize a figure of merit based on the error ε_n typically the sum-squared error [1]. The function $\beta(\cdot)$ is a know function to match the properties of the reference stimuli r_n to the level of the signal analyzer output s_n. With reference to Figure 2.3, the resulting baseband signal s_n should typically have the same spectral support as the reference signal r_n.

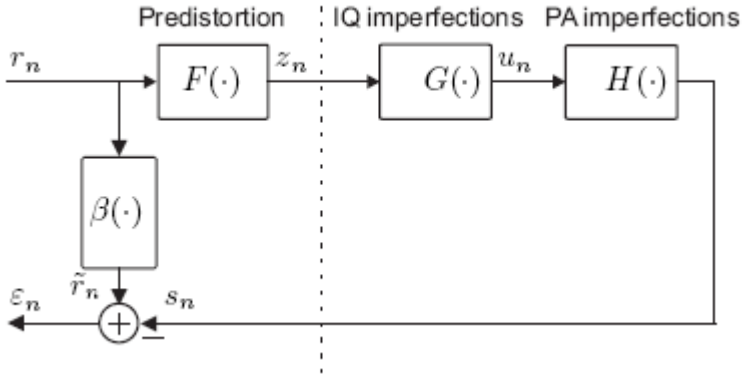

Figure 2.3. Baseband equivalent

In order to handle the inherent delays in the measurement, ideally the signal generator output equals

$$s_n = \alpha e^{i\Phi} r_{n-k} \qquad (2.1)$$

that is, the analyzer baseband output is an attenuated or amplified (by the real valued factor α >0) delayed (by *k* samples) and phase-shifted (ϕ radians) replica of the baseband reference signal r_n . In order to simplify the notation, introduce the normalized reference signal $\tilde{r}_n$ as

$$\tilde{r}_n = \beta(r_n) \qquad (2.2)$$

where, for example, $\beta(r_n) = \alpha e^{i\phi} r_{n-k}$.

2.4 Pre-distorter design based on physical modelling

There is a basic observation in the identification system to look for the physical process of improving the quality of models derived. Predistortion in almost a linear or vaguely non-linear, dynamic systems can be performed by a variety of model structures. Here, we rely on the physical behavioural and study a clear impact on the IQ imbalance and deficiencies of the amplifier between the nonlinearities of the main sources for this type of equipment. In such a way, physically motivated structures for predistorter design are achieved. The aim of this section is to derive the structure of the Parsimonious parameterized digital predistorter [1]. Then, in Section, 2.7 we focus on training of the derived predistorter.

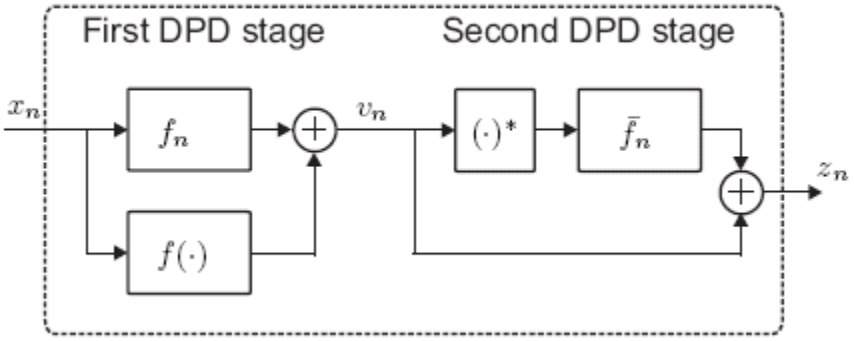

Figure 2.4. Digital predistortion design

Figure 2.4 shows digital predistorter design where input signal x_n produces the output signal z_n. In operational mode $x_n = r_n$ (see Figure 2.3) producing output z_n and in calibration mode $x_n = s_n$ (see Figure 2.7) producing $\hat{z}_n$, respectively.

The function f_n and $\bar{f}_n$ are pulse responses, $f(\cdot)$ denotes the nonlinear branch of the parallel Hammerstein structure, and $(\cdot)^*$ denotes conjugate operation. Conceptually, we employ a cascade structure of the digital pre-distorter, see Figure 2.4 the first stage of the predistorter is designed to deal with imperfections in the power amplifier and the second stage the imperfections in the IQ modulator, so that ideally for $\beta(r_n) = r_n$ in (2.2) the distorter output in operational mode is given by

$$z_n = F(r_n) = G^{-1}\left(H^{-1}(r_n)\right) \tag{2.4}$$

yielding

$$s_n = H\left[G(z_n)\right] = H\left\{ G\left[G^{-1}\left(H^{-1}(r_n)\right)\right] \right\} = r_n \tag{2.5}$$

under an assumption that the involved inverses exist.

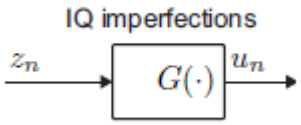

Figure 2.5. IQ imperfection in the signal generator

2.4.1 IQ imbalance

IQ imbalance mainly attribute to the mismatched components in the I and the Q branches. Examples include but not limited to an imperfectly balance local oscillator and/or baseband low pass filters with mismatch frequency responses [11]. The digital pre-distortion design in Figure 2.4 will give improvement to the IQ imbalance. In Figure 2.3 the baseband equivalent of the IQ modulator output by u_n. Due to the IQ imbalance we have that u_n of the IQ modulator output is given by [12]:

$$u_n = g_n * z_n + \overline{g}_n * z_n^* \qquad (2.6)$$

g_n and $\overline{g}_n$ are some unknown linear time invariant pulse responses. The physical interpretation of the pulse responses is referred to [12]. A detailed discussion on the topic is available in [4]. The model in (2.6) captures the IQ mixer amplitude and phase imbalance, impulse response due to the digital-analog conversion (DAC) and analog low-pass filters. The model is flexible enough to capture the behaviour of frequency dependent IQ imbalance, as well. The second term in (2.6) is the mirror distortion. With z_n being a complex-valued cisoid $z_n = e^{jw_0 n}$, the IQ modulator outputs both an amplitude and phase shifted cisoid with angular frequency ω_0, but also a component at angular frequency $-\omega_0$.

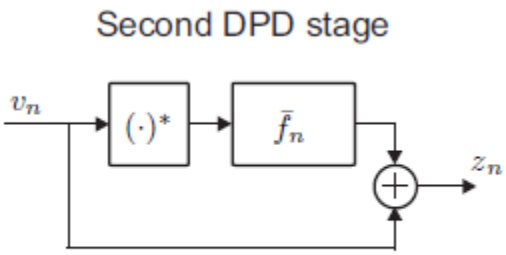

Figure 2.6. Digital predistortion design for IQ imbalance

The IQ imbalance is to be compensated by the second stage of the predistorter. With reference to Figure 2.6, we consider the second stage of the predistorter defined by its input v_n and output z_n given by:

$$z_n = v_n + \bar{f}_n * v_n^* \tag{2.7}$$

where $\bar{f}_n$ is the pulse response of a linear time invariant filter. We have chosen to exclude a linear filter operating on the first term in (2.7), a filter that without loss of generality can be include in the first stage of the predistorter. The second stage output (2.7) results in an IQ modulator output u_n in (2.6) given by:

$$\begin{aligned} u_n &= g_n * \left(v_n + \bar{f}_n * v_n^*\right) + \bar{g}_n * \left(v_n + \bar{f}_n * v_n^*\right)^* \\ &= \left(g_n + \bar{g}_n * \bar{f}_n^*\right) * v_n + \left(g_n * \bar{f}_n + \bar{g}_n\right) * v_n^* \end{aligned} \tag{2.8}$$

The mirror distortion is cancelled by forcing the second term in (2.8) or $g_n * \bar{f}_n + \bar{g}_n$ to zero for all time instants n, by a proper selection of the predistorter coefficients gathered in $\bar{f}_n$ [12]. For the subsequent discussion, it is assumed that the second stage of the predistorter is perfectly tuned. That is, subject to cancelled mirror distortion one has that the input to the power amplifier is a filtered replica of v_n:

$$u_n = a_n * v_n \tag{2.9}$$

For a pulse response a_n implicitly given by $a_n = g_n + \bar{g}_n * \bar{f}_n^*$ subject to the condition $g_n * \bar{f}_n + \bar{g}_n = 0$, that is $a_n = g_n * \left(1 - \bar{f}_n * \bar{f}_n^*\right)$. Under the null-mirror-distortion assumption the structure for the first stage of the predistorter for power amplifier deficiencies is discussed in Section. 2.4.3.

2.4.2 Predistortion mirror distortion

In order to determine the parameter values of the digital predistorter, the training set-up in Figure 2.7 is considered. With reference to Figure 2.7, the model output $\hat{z}_n$ describing the inverse of the IQ imbalance reads

$$\hat{z}_n = s_n + \bar{f}_n * s_n^* \qquad (2.10)$$

The objective in this section is to formulate the least-squares problem to obtain the parameters of the unknown pulse response $\bar{f}_n$. Thus,

$$\bar{z}_n \overset{\Delta}{=} \hat{z}_n - s_n = \bar{f}_n * s_n^* \qquad (2.11)$$

Consider N samples of the user generated stimuli z_n resulting in the corresponding signal analyzer output s_n, that is data $\{z_0, \cdots, z_{N-1}\}$ and $\{s_0, \cdots, s_{N-1}\}$, respectively. Denote the column vectors with the sought for predistorter pulse response by $\bar{f}$. Then, the predictor output $\bar{z} = \hat{z} - s$ with $\bar{z} = \left(\bar{z}_0, \ldots, \bar{z}_{N-1}\right)^T$ (where T denotes transpose) can be written

$$\bar{z} = s_0^* \bar{f} \qquad (2.12)$$

where s_0 in (2.12) is given by

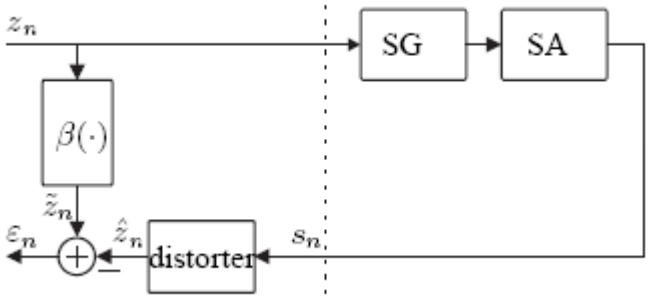

Figure 2.7. Training of the digital predistorter $F(s_n;\theta)$

$$s_0 = \begin{pmatrix} s_0 & 0 & \cdots & 0 \\ s_1 & s_0 & & \vdots \\ \vdots & & \ddots & 0 \\ s_L & \cdots & & s_0 \\ \vdots & & & \vdots \\ s_{N-1} & \cdots & & s_{N-L-1} \\ 0 & \ddots & & \vdots \\ \vdots & & s_{N-1} & s_{N-2} \\ 0 & \cdots & 0 & s_{N-1} \end{pmatrix} \qquad (2.13)$$

With $\tilde{z} = \beta(z)$ defined by (2.2), the least-squares solution $\hat{\tilde{f}} = \arg\min \left\| \tilde{z} - \bar{z} \right\|_2$ reads

$$\hat{\tilde{f}} = \left(s_0^H s_0^* \right)^{-1} s_0^H \bar{z} \qquad (2.14)$$

Leading to the predistorter in operation

$$z_n = r_n + \hat{\tilde{f}} * r_n^* \qquad (2.15)$$

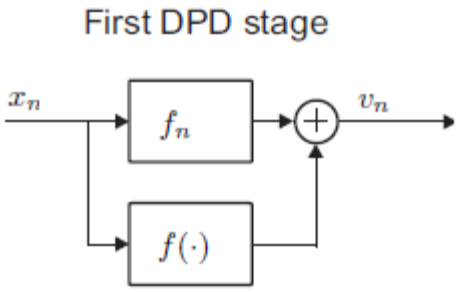

Figure 2.8. Digital predistortion design for power amplifier

2.4.3 Power amplifier deficiencies

In order to minimize nonlinear distortion that produced from the power amplifier, digital predistortion was applied to the signal generator to correct the nonlinearities and cancel distortion introduced by power amplifier. In digital predistortion the signal is distorted in the digital domain to compensate for the power amplifier's signal distortion. In model based digital predistortion an approximate inverse of the PA's transfer function is used [13]. The first stage of the predistorter handles the nonlinear artifacts introduced by the power amplifier. A digital predistortion was used to generate an input signal to the power amplifier to reduce the non-linear region in the amplifier. A parallel Hammerstein or memory polynomial models are used for inverse as well as direct modelling of power amplifiers subject to memory effects [14]. The employed predistorter has the form of a parallel Hammerstein model that is consists of the nonlinearity followed by a linear filter is often used to present certain higher-order nonlinear systems, which input-output relation formally can be written as reference to Figure 2.8.

$$v_n = f_n * x_n + f(x_n) \qquad (2.16)$$

where f_n is the pulse response of the linear time invariant filter of the linear path in the

parallel Hammerstein structure. The function $f(x_n)$ is a short notation for the sum of the nonlinear branches. In this project, both the traditional parallel Hammerstein structure with odd order polynomial coefficients has been considered, that is

$$f(x_n) = \sum_{m=1}^{M} f_{m,n} * \left(|x_n|^{2m} x_n \right) \qquad (2.17)$$

From (2.17), we note that each branch (that is, for each *m= 1,…, M*) is described by linear filtering (determined by the filter coefficients $\{ f_{m,1}, \ldots , f_{m,M} \}$) of the input $|x_n|^{2m} x_n$ for all n. Introduce $\phi_m(x_n) = |x_n|^{2m} x_n$ for *m=1,…, M,* then (2.17) reduces to

$$f(x_n) = \sum_{m=1}^{M} f_{m,n} * \phi_m(x_n) \qquad (2.18)$$

The basis functions $\phi_m(\cdot)$ are summarized in Table I.

Table I

Basis function for a conventional parallel Hammerstein model (memory polynomial) $\phi_m(x)$ respectively the complex-valued counterpart to the shifted Legendre polynomials $\psi_m(x)$ [15].

m	$\phi_m(x)$	$\psi_m(x)$
1	$\|x\|^2 x$	$4\|x\|x - 3x$
2	$\|x\|^4 x$	$15\|x\|^2 x - 20\|x\|x + 6x$
3	$\|x\|^6 x$	$56\|x\|^3 x - 105\|x\|^2 x + 60\|x\|x - 10x$
4	$\|x\|^8 x$	$210\|x\|^4 x - 504\|x\|^3 x + 420\|x\|^2 x - 140\|x\|x + 15x$

For a robust implementation, numerical aspects have to be taken into account. For that purpose, the basis functions in [15] are employed as well. Thus the basis function $\phi_m(\cdot)$ in (2.18) is replaced by $\psi_m(\cdot)$ given by the complex-valued counterpart to the shifted Legendre polynomials [15]:

$$\psi_m(x) = \sum_{\ell=1}^{m+1} \frac{(-1)^{\ell+m+1}(m+1+\ell)!}{(\ell-1)!(\ell+1)!(m+1-\ell)!} |x|^{\ell-1} x \qquad (2.19)$$

Table I shows the four orthogonal polynomials for $\psi_m(\cdot)$. If we replace the complex valued basis functions $|x|^{m-1}x,\ m = 1,2,.....,m$ with real-valued basis function $|x|^m,\ m = 1,2,....,m$, the real valued orthogonal polynomials defined in the region [0, 1], which are known as the shifted Legendre polynomial, except that the $|x|^0$ polynomial is not included. The construction of an orthogonal basis is often an iterative procedure. One may note that $\phi_m(\cdot)$ only contains odd powers of x_n, whereas $\psi_m(\cdot)$ also includes even powers.

2.5 Parsimonious predistorter structures

Parsimonious predistorter structure used in this project, the predistorter $F(\cdot)$ in Figure 2.3 consists of three filtering blocks, namely the linear time invariant filtering by f_n of the input x_n, the linear time invariant filtering by $\bar{f}_n$ of the conjugate of the first-stage output v_n, and the *M* branches of time invariant linear filtering by the $\{f_{m,n}\}_{m=1}^{M}$ of the static nonlinear mapping of the input x_n by the appropriate basis function $\phi_m(\cdot)$ and $\psi_m(\cdot)$, respectively. Accordingly, the design objective of the predistorter is to find the suitable parameters of the pulse responses f_n, $\bar{f}_n$ and $f_{1,n,\cdots,} f_{M,n}$ where the integer *M* and the lengths of the individual pulse responses are still to be determined (in a structural way). Combination of (2.7) and (2.19), rearranging terms yields

$$z_n = f_n * x_n + \underbrace{\bar{f}_n * f_n^*}_{f_n'} * x_n^* + f(x_n) + \bar{f}_n * f(x_n)^* \qquad (2.20)$$

where the pulse response f_n' is introduced to simplify the notation. Divide z_n in (2.20) into its linear and nonlinear parts, viz as [1].

$$z_n = z_n^L + z_n^N \qquad (2.21)$$

where by definition

$$z_n^L = f_n * x_n + f_n' * x_n^* \qquad (2.22)$$

and

$$z_n^N = f(x_n) + \bar{f}_n * f(x_n)^* \qquad (2.23)$$

The linear (2.22) and nonlinear (2.23) parts are analyzed in the following sections.

2.5.1 Linear part of the predistorter

In the linear part of the predistoerter, there is no overlap in the spectral support of the source and its mirror distortion. Accordingly, there is an ambiguity in the linear part in (2.22). This fact is clearly seen by transforming the model to the frequency domain. The frequency domain representation of (2.22) is given by $F(\omega)X(\omega) + F'(\omega)X^*(-\omega)$, where $F(\omega), F'(\omega)$ and $x(\omega)$ are the Fourier transform of the corresponding time domain quantities. For a cisoid input $x_n = \exp(i\omega_0 n)$ with frequency ω_0, the output signal is given by $F(\omega_0)\exp(i\omega_0 n) + F'(-\omega_0)\exp(-i\omega_0 n)$, where the gains and phase-shifts are determined by $F(\omega_0)$ and $F'(-\omega_0)$, respectively.

In a similar vein, the output from another filter, say $H'(\omega)$, driven by the sum $\exp(i\omega_0 n) + \exp(-i\omega_0 n)$ follows by the superposition's principle as $H'(\omega_0)\exp(i\omega_0 n) + H'(-\omega_0)\exp(-i\omega_0 n)$. Accordingly, we cannot distinguish the two separate branches determined by $F(\omega)$ and $F'(\omega)$ and the single branch determined by $H'(\omega)$, with $H'(\omega_0) = F(\omega_0)$ and $H'(-\omega_0) = F'(-\omega_0)$. Accordingly, for a parsimonious model structure we replace the two pulse responses f_n and f'_n in (2.22) with h'_n [1], viz.

$$z_n^L = h'_n * \left(x_n + \gamma\, x_n^*\right) \tag{2.24}$$

The scalar γ in (2.24) is a complex –valued scaling and rotation. The wisdom of γ is to reduce the dynamic range of the transfer function corresponding to the pulse response h'_n. Intuitively, the magnitude of γ should be chosen proportional to the actual mirror distortion of the signal generator, that is the injected mirror component $\gamma\, x_n^*$ produced by the predistorter should be of the same magnitude as the actual mirror distortion of the signal generator. Furthermore, it is necessary that the coefficient of the pulse response corresponding to the direct term, which is the term at time instant *n* equals unity since the scaling is taken care of by $\beta(\cdot)$ in (2.2). In order to manage imbalance in the tuning of $\beta(\cdot)$ the pre-distorter consist of a direct term, that is (2.24) is replaced by

$$z_n^L = x_n + h_n * \left(x_n + \gamma\, x_n^*\right) \tag{2.25}$$

where the requirement on a unity direct term in the pulse response h_n is relaxed.

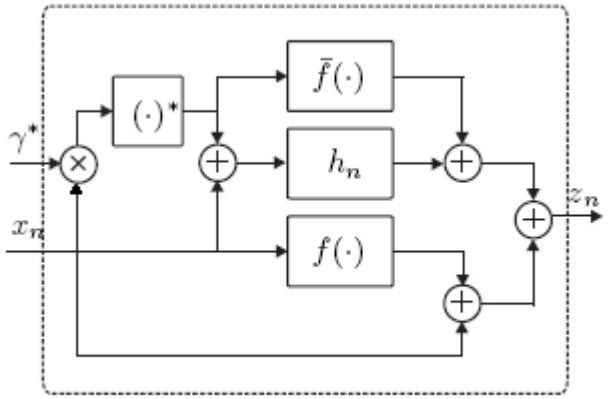

Figure 2.9. Digital predistorter where input signal x_n produces output signal z_n.

2.5.2 Non linear part of the predistorter

The nonlinear part z_n^N in (2.23) is analyzed to find a parsimonious representation. In fact, it is sufficient to analyze the second term in (2.23), that is

$$\bar{f}_n * f(x_n)^* = \bar{f}_n * \left(\sum_{m=1}^{M} f_{m,n} * \Phi_m(x_n) \right)^* \qquad (2.26)$$

where the equality follows from (2.18). A rearrangement of terms yields

$$\bar{f}_n * f(x_n)^* = \sum_{m=1}^{M} \bar{f}_n * f_{m,n}^* * \Phi_m(x_n)^* \qquad (2.27)$$

where the pulse responses $\bar{f}_{m,n} = \bar{f}_n * f_{m,n}^*$ for *m=1,…, M* are introduced to simplify the notation. Further, we note that our basis function $\Phi_m(x)$ (and $\psi_m(x)$) obey $\Phi_m(x)^* = \Phi_m(x^*)$ (and $\psi_m(x)^* = \psi_m(x^*)$). Thus, (2.27) is reduced to

$$\bar{f}_n * f(x_n)^* = \sum_{m=1}^{M} \bar{f}_{m,n} * \Phi_m(x_n^*) \qquad (2.28)$$

One may note that the right side of (2.28) exactly has the same structure as (2.18), but for some other parameter values $\bar{f}_{m,n}$. Therefore we can write the right hand side of (2.28) as $\bar{f}(x_n^*)$, where $\bar{f}(x_n^*)$ satisfy (2.18). In summary, gathering the derived results (2.21), (2.24), (2.28) the predistorter is parsimoniously described by [1]

$$z_n = x_n + h_n * (x_n + \gamma\, x_n^*) + f(x_n) + \bar{f}(\gamma\, x_n^*) \qquad (2.29)$$

where $f(\cdot)$ and $\bar{f}(\cdot)$ are nonlinearities according to (2.18) (eventually with $\phi_m(\cdot)$ in (2.18) replaced by $\psi_m(\cdot)$) with two different set of parameter values. We notes that the scaling γ has been introduced in $\bar{f}(\cdot)$, again motivated by the difference in power between the direct path and the conjugate path. The resulting predistorter structure is given by Figure 2.9.

2.6 Predistorter properties

The predistorter input-output relation that introduced in (2.4) is written as

$$z_n = F(x_n;\theta) \qquad (2.30)$$

where x_n is the input signal, and z_n the output, θ is introduced as a generic parameter vector of proper length. The entries of θ consist of the parameter of the gain γ and sought for pulse responses h_n, $f_{m,n}$ and $\bar{f}_{m,n}$ for $m = 1,\ldots, M$, where $f_{m,n}$ and $\bar{f}_{m,n}$ are defined through (2.18). The following properties of $F(x_n;\theta)$ is:

$$\text{Property 1: } F(x_n;0) = x_n \qquad (2.31)$$

where 0 is the null-vector of appropriate size. The implication of (2.31) is that generator-analyzer set-up that only introduces a gain and phase shift. Let x_n be a cisoid $x_n = \exp(iw_0 n)$, then it holds that:

$$\text{Property 2: } F\left(e^{i\omega_0 n};\theta\right) = c_1 e^{iw_0 n} + \gamma c_2 e^{-iw_0 n} \qquad (2.32)$$

c_1 and c_2 is the complex – valued constants. The implication of (2.32) is that a predistorter linear in $x_n + \gamma x_n^*$ is sufficient for signal tone stimuli, that is $M = 0$. Another property includes the least-squares training properties given in Section 2.7

$$\text{Property 3a: } \hat{\theta} = \arg\min_{\theta} V(\theta) \qquad (2.33)$$

where

$$\text{Property 3b: } V(\theta) = \sum_{n=0}^{N-1} \left(\beta(z_n) - F(s_n,\theta)\right)^2 \qquad (2.34)$$

where N is the number of collected samples in the training phase, z_n is the input stimuli to the signal generator, and s_n is the baseband output from the signal analyzer; see Figure 2.7.

$$\text{Property 4: } V\left(\hat{\theta}_\ell\right) \le V\left(\hat{\theta}_{\ell-1}\right) \qquad (2.35)$$

where ℓ denotes the number of parameters in θ. Due to the nonlinearities involved carefulness is required in the process of model order selection and number of parameters in the different filter branches.

2.7 Training of the predistorter based on N-sequences of data

To determine the values of the parameters of the digital predistorter, the training set-up in Figure 2.7 is considered. In Figure 2.7, $\beta(\cdot)$ is assumed known.

In this Section the least- squares problem is formulated and studied subject to a given structure that is subject to a given set of parameters that are included in the generic parameter vector θ.

2.7.1 Model output

The model output $\hat{z}_n$ with reference to Figure 2.7 describing the inverse of the chain of equipment reads

$$\hat{z}_n = s_n + h_n * \left(s_n + \gamma s_n^*\right) + f\left(s_n\right) + \bar{f}\left(\gamma s_n^*\right) \qquad (2.36)$$

The aim of this section is to formulate a least squares problem to obtain the unknown pulse response h_n, $f_{m,n}$ and $\bar{f}_{m,n}$ for $m = 1,\ldots,M$, where $f_{m,n}$ and $\bar{f}_{m,n}$ implicitly are defined through (2.18). We introduce the simplified notation for the different transformed versions of the output of the signal analyzer s_n, that is the sum of the signal and it's conjugate

$$\bar{s}_n = s_n + \gamma\ s_n^* \qquad (2.37)$$

and the nonlinear static mappings of s_n, that is

$$s_{m,n} = \phi_m\left(s_n\right) \qquad (2.38)$$

and

$$\bar{s}_{m,n} = \phi_m\left(\gamma s_n^*\right) \qquad (2.39)$$

with the notation (2.37)-(2.40), the model output (2.36) is rewritten as

$$\hat{z}_n - s_n = h_n * \bar{s}_n + \sum_{m=1}^{M} f_{m,n} * s_{m,n} + \sum_{m=1}^{M} \bar{f}_{m,n} * \bar{s}_{m,n} \qquad (2.40)$$

Let the order of the linear filters be L, that each filter comprises $L+1$ filter coefficients. This is not an absolute requirement, but makes the notation significantly less complex. The number of nonlinear branches M in $f(\cdot)$ and $\bar{f}(\cdot)$ is, at the moment equal.

Then, one may then note that the total number of coefficients to be estimates is $(2M + 1)(L + 1)$. For example, with tenth order filters and 2+2 nonlinear branches, there are some 55 complex-valued parameters to estimate. Then, write out the explicit form of the convolutions, the predistortor output reads

$$\bar{z}_n = \sum_{\ell=0}^{L} h_\ell \bar{s}_{n-\ell} + \sum_{m=1}^{M} \sum_{\ell=0}^{L} f_{m,\ell} s_{m,n-\ell} + \bar{f}_{m,\ell} \bar{s}_{m,n-\ell} \qquad (2.41)$$

where we also introduced $\bar{z}_n = \hat{z}_n - s_n$. Consider N samples of the user generated stimuli z_n resulting in the corresponding signal analyzer output s_n, that is data $\{z_0, \ldots, z_{N-1}\}$ and $\{s_0, \ldots, s_{N-1}\}$, respectively. Denote the column vectors (still, all of length $L+1$) with the sought for predistorter pulse responses by $h, f_1, \ldots, f_M, \bar{f}_1, \ldots, \bar{f}_M$, and left f and $\bar{f}$ be the augmented column vectors of length $M(L+1)$, given by:

$$f = \begin{pmatrix} f_1 \\ \vdots \\ f_M \end{pmatrix} \qquad (2.42)$$

and

$$\bar{f} = \begin{pmatrix} \bar{f}_1 \\ \vdots \\ \bar{f}_M \end{pmatrix} \qquad (2.43)$$

Then, the predictor output $\bar{z} = \hat{z} - s = (\bar{z}_0, \ldots, \bar{z}_{N-1})^T$ (where T denotes transpose) can be written

$$\bar{z} = \begin{pmatrix} \bar{s} & S & \bar{S} \end{pmatrix} \begin{pmatrix} h \\ f \\ \bar{f} \end{pmatrix} \qquad (2.44)$$

where $\bar{s}$ in (2.44) is given by $\bar{s} = s_0 + \gamma s_0^*$ where

$$s_0 = \begin{pmatrix} s_0 & 0 & \cdots & 0 \\ s_1 & s_0 & & \vdots \\ \vdots & & \ddots & 0 \\ s_L & \cdots & & s_0 \\ \vdots & & & \vdots \\ s_{N-1} & \cdots & & s_{N-L-1} \\ 0 & \ddots & & \vdots \\ \vdots & & s_{N-1} & s_{N-2} \\ 0 & \cdots & 0 & s_{N-1} \end{pmatrix} \qquad (2.45)$$

Further, **S** in (2.44) (of size $(N+L)\times M(L+1)$) and its companion s^* are data matrices formed from the signal generator output. Explicitly, **S** is composed out of M + 1 sub-matrix as:

$$\mathbf{S} = (s_1 \cdots s_M) \qquad (2.46)$$

where s_m is the of size $(N+L)\times(L+1)$ Toeplitz data matrix (for *m = 1,…,M*):

$$s_m = \begin{pmatrix} s_{m,0} & 0 & \cdots & 0 \\ s_{m,1} & s_{m,0} & & \vdots \\ \vdots & & \ddots & 0 \\ s_{m,L} & \cdots & & s_{m,0} \\ \vdots & & & \vdots \\ s_{m,N-1} & \cdots & & s_{m,N-L-1} \\ 0 & \ddots & & \vdots \\ \vdots & & s_{m,N-1} & s_{m,N-2} \\ 0 & \cdots & 0 & s_{m,N-1} \end{pmatrix} \tag{2.47}$$

where $s_{m,n}$ was introduced in (2.38). The matrix $\bar{s}$ is constructed in a similar vein replacing $s_{m,n}$ in (2.47) with $\bar{s}_{m,n}$ as defined in (2.40) [1].

2.7.2 Least-squares problem

Method of least squares or ordinary least squares (OLS) is used to solve the over determined system that is a system of approximately linear equations. Least square is often applied in statistical context, particularly regression analysis. The method was first described by Johann Carl Friedrich Gauss around 1794.

Least squares can be interpreted as a method of fitting data the best fit in the Least-squares sense is that instance of the model for which the sum of squared residuals has its least value, a residual being the difference between an observed value and the value given by the model. In this work, the least-squares solution of the predistorter coefficients is given by minimizing $\left\|\tilde{z} - \bar{z}\right\|^2$. From the vector $\tilde{z}$ given by (2.2), i.e. $\tilde{z} = \beta(z)$. In short, the linear set of equations reads

$$\underbrace{\begin{pmatrix} \bar{s} & S & \bar{S} \end{pmatrix}}_{R(\gamma)} \quad \underbrace{\begin{pmatrix} h \\ f \\ \bar{f} \end{pmatrix}}_{\theta} = \tilde{z} \tag{2.48}$$

Here, the dependency of **R** on the scaling γ is explicitly indicated.

2.7.3 Determination of the function $\beta(\cdot)$

The source signal r_n in Figure 2.3 is a complex - valued wide sense stationary process with auto-correlation function $R_p = E\left[r_{n+p} r_n^*\right]$, R_0 is the signal power σ_r^2. Then, the cross-correlation between the signal generator output s_n and the reference signal r_n, that is $S_p = E\left[s_{n+p} r_n^*\right]$ directly follows from (2.1) as $S_p = \alpha e^{i\phi} E\left[r_{n-k+p} r_n^*\right]$. The inherent delay *K* in (2.1) is found as the bin location of the maxima of $|S_p|$, that is

$$K = \arg\max_P |S_P| \qquad (2.49)$$

For the sought for *K* given by (2.49), it holds that the cross-correlation yields

$$S_{p=k} = \alpha e^{i\varphi} \sigma_r^2 \qquad (2.50)$$

Accordingly, the real-valued and positive quantity α can be determined by peak picking the maximum magnitude value of the cross-correlation normalized with the power of the source signal, that is $\alpha = \left|S_{p=k}\right| / \sigma_r^2$. The phase follows by $\varphi = \angle\left[S_{p=k}\right]$. In practice, the cross-correlation S_p and power σ_r^2 are replaced by the corresponding estimated quantities based on measured data [1].

3 Method

3.1 Introduction

This Chapter presented the technical and theoretical information that was used to have the appropriate test setup, simulation and measurement procedure. It includes an overview of the test setup, implemented system, measurement system, internal structure and configuration of the different instruments used in this work for generating spectrally pure signal. It consists of the simulation model and parameter determination that is consists of the gamma (γ), model order M and L, basis function $\psi_m(\cdot)$ or $\phi_m(\cdot)$ and realization. The device under test was the IQ modulation mismatch and amplifier deficiencies in the signal generator Rhode & Schwarz SMU200A. The design digital pre-distortion that is implemented in software so that the dynamic range of the signal generator output after pre-distortion is superior to that of the output prior to it.

3.2 Test Setup

We consider measurement set-ups where the signal generator is synchronized with the signal analyzer. The test setup consists of a Rhode & Schwarz SMU200A Generator, a Rhode & Schwarz FSQ 26 Signal Analyzer, and a personal computer interconnected to arrange an appropriate measurement environment for the DUT characterization, these instruments are essential for the generating a spectrally pure signals.

3.2.1 The implemented system

We consider the set-up in Figure 3.1 where the digital arbitrary wave-form baseband test stimuli z_n (a complex - valued quantity) is generated by software and transmitted in digital format to the signal generator for DAC of the in-phase and quadrature branches,

followed by a modulation wheel to produce the analog radio frequency signal r_t. In the calibration set-up, the signal generator radio frequency output r_t is connected directly to the input of the signal analyzer, producing the down- converted baseband signal s_n of the radio signal.

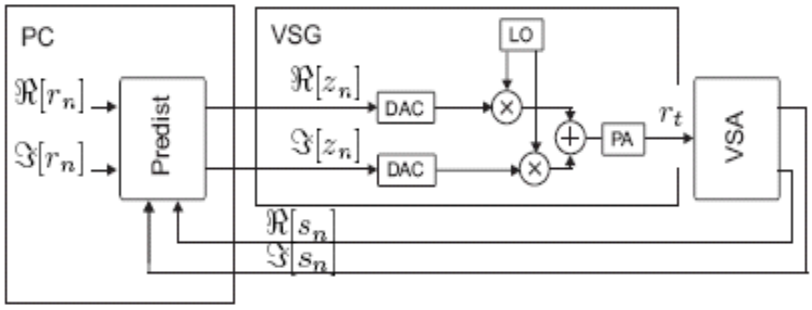

Figure 3.1. Calibration set-up.

By the design of a predistorter a high quality radio frequency output r_t will produce to calculate the proper stimuli z_n by nonlinear dynamic filtering of a baseband reference r_n. In other words, r_n is the desired baseband representation of the radio frequency signal r_t. The notation $\Re[\cdot]$ and $\Im[\cdot]$ denote the real and imaginary part of the complex-valued quantity within the brackets. The quality measure is typically directly related to the squared error, where the error is defined as the difference between a reference, or target, signal and the feedback baseband signal s_n. It is assumed that the performance of the analyzer is superior to that of the generator, and that the instruments are synchronized, both during the phase of calibration and the subsequent measurement campaign. The device under test is the IQ imbalance and power amplifier deficiencies in the signal generator. Due to the derived digital predistortion function the signal generator now behaves as a better performance to excite the device under test.

3.2.2 Vector Signal Generator (VSG)

The R&S SMU 200A vector signal generator used in this measurements, that had two DAC each with clock frequencies up to 100 MHz and it was equipped with an AWG, with IQ modulation. In this work, the two-tone baseband signal where generated in Matlab program, all the different parameters were specified, such as amplitude, frequency and phase difference between I and Q. Coherent sampling was used to ensure higher spectral resolution. The signal was generated in Matlab as I and Q data files and down loaded to the AWG. The AWG generates the analogue I and Q signals at baseband as

$$I(t) = \sum_{K=1}^{N} A_k(t)\cos\left(w_k t + \phi_k(t) + \varphi_k\right) \tag{3.1}$$

$$Q(t) = \sum_{K=1}^{N} A_k(t)\sin\left(w_k t + \phi_k(t) + \varphi_k\right) \tag{3.2}$$

Where A_k, ϕ_k, w_k and φ_k are the amplitude, phase, frequency and initial phase of the k:th sub-carrier [16]. The I and Q signals are then fed to the IQ-modulator in the signal generator. The modulation is described in (3.3), the output of the modulator is represent by $s(t)$

$$s(t) = r(t)\cos(w_c t + \varphi(t)) \tag{3.3}$$

where w_c is the carrier frequency and:

$$r(t) = \left(I^2(t) + Q^2(t)\right)^{1/2} \tag{3.4}$$

$$\varphi(t) = \arctan\left(\frac{I(t)}{Q(t)}\right) \tag{3.5}$$

The signal $r(t)$ is the envelope of $s(t)$ and $\varphi(t)$ is the phase of $s(t)$ [17].

3.2.3 Vector Signal Analyzer (VSA)

The R&S FSQ26 vector signal analyzer used in this project that has an IQ demodulator that returns the values of the signals in a complex format, Figure 3.2 shows the analyzer hardware.

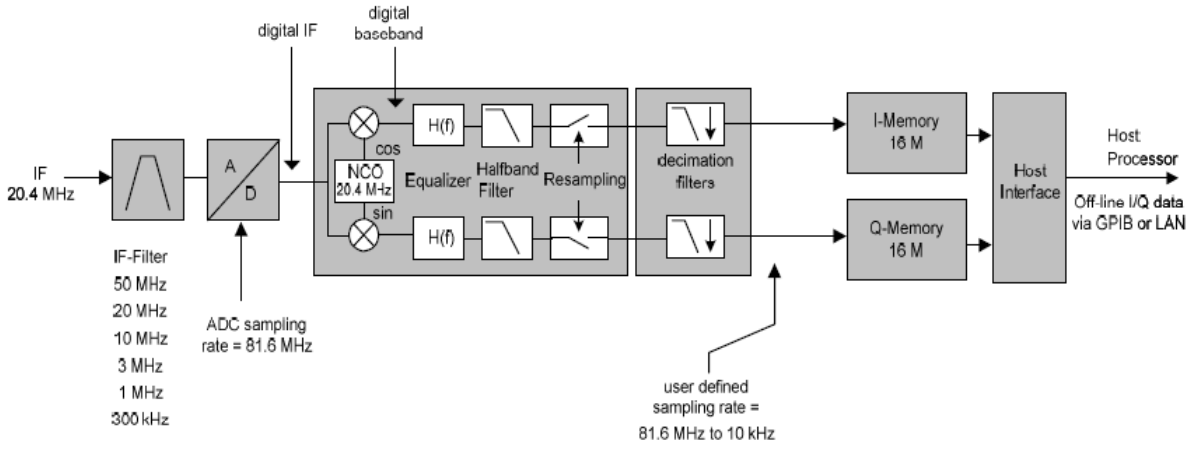

Figure 3.2. Hardware from IF to the process [18].

The radio frequency input signal is down-converted to an intermediate frequency (IF) of 20.4 MHz. The IF signal is digitized using ADC with 81.6 MHz sampling rate. An analog bandpass filter in front of the ADCs limits the spectrum. The digitized (IF) is down-converted to IQ baseband using a digital mixer fed by a numerical controlled oscillator (NCO). The digital equalizer filter corrects the amplitude and phase distortion. Then the signal resample's which reduces the sampling rate from 81.6 MHz to 40.8 MHz to adapt the actual signal bandwidth. Finally the output sampling rate can be adjusted from 81.6 MHz to 10 KHz. Then the IQ signal is filtered by low pass filters and written continuously into the IQ memory in parallel. Most of the functions in the VSA can be control from a program Matlab, for example resolution bandwidth (RBW), video bandwidth (VBW), Reference level (Ref), attenuation (Att) and span.

3.3 Simulation model

The simulation model comprises of an IQ imbalance given by first order linear filtering, and a power amplifier model described as a parallel Hammerstein system. White Gaussien noise is added to the IQ modulator output, and is thus propagated through the parallel Hammerstein model. Each filter in the parallel Hammerstein model consist of three filter taps employing a two tone stimuli with positive frequencies.

A parsimonious predistorter structure has been used in this project that is consisting of three filtering blocks, with reference to Figure 2.9. Where $f(\cdot)$ and $\bar{f}(\cdot)$ are nonlinearities according to (2.18) and h_n is the pulse response of the linear time invariant filter. We consider the relation introduced in Figure 2.9. the signal x_n is the complex input signal, and z_n the output signal. A generic parameter vector θ is introduced as a proper length. The entries of θ consist of the parameters of the gain γ and sought for pulse response h_n, $f_{m,n}$ and $\bar{f}_{m,n}$ for $m = 1,...,M$, where $f_{m,n}$ and $\bar{f}_{m,n}$ implicitly are defined through (2.18). The least squares problem has used to obtain the parameters of the unknown pulse response h_n, $f_{m,n}$ and $\bar{f}_{m,n}$ for $m = 1,...,M$. The least squares problem have calculated from equation (2.48), the equation (2.37) has been calculated and then S and $\bar{S}$ matriser have been determined. We have used basis function $\phi_m(\cdot)$ to generate the simulation signal, then we have used basis function $\psi_m(\cdot)$ to generate it.

3.4 Determinate parameters

3.4.1 Gamma (γ)

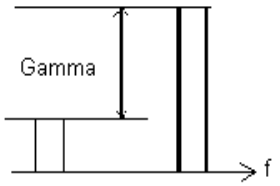

Figure 3.3. Gamma (γ)

The scalar γ is a complex-valued scaling and rotation. The rational for using γ is to reduce the dynamic range of the transfer function. The magnitude of γ has been chosen proportional to the actual mirror distortion of the signal generator. The γ has been chosen from the measuring data between a two-tone signal and the mirror distortion that we had, with reference to Figure 3.3.

3.4.2 Model order

The model order L is the linear filter that each filter comprises $L+1$ filter coefficients and the model order M is the number of nonlinear branches in $f(\cdot)$ and $\bar{f}(\cdot)$ at the moment equal. In the theory parts says that we should calculate $V(\theta)$ from (2.34) for different values of M and L. Then we should make a three dimensional plots. The parameter values of M and L, which gave the lowest value of $V(\theta)$, we will chose as the best parameter choice. Because of problems with numerical solutions so unfortunately this has not been implemented in practice

3.4.3 Basis function $\psi_m(\cdot)$ or $\phi_m(\cdot)$

The polynomial model is communly used in power amplifier modeling and predistorter design. Higher order polynomials present a challenge for both power amplifier modelling and predistortion design. However, the basis function $\phi_m(\cdot)$ (see Section 2.4.3) exhibits numerical instabilities when higher order terms are included. Theoritically, the basis function $\phi_m(\cdot)$ or $\psi_m(\cdot)$ are equivalent and thus should behave similarly. In practise, the two approaches can perform quite differently in the presence of finite precision processing[15]. One may note that basis function $\phi_m(\cdot)$ only contains odd powers of the input signal x_n, whereas basis function $\psi_m(\cdot)$ also includes even power. we have tested both models to evaluate which is most appropriate. So, the basis function $\psi_m(\cdot)$ had a better performance than the basis function $\phi_m(\cdot)$.

3.4.4 Realization

In this project, it was a shortage of mathematics, because we calculated $\bar{S}$ matrix with γ. Since γ is a small speech, then all columns in $\bar{S}$ will be small compared to the columns of S matrix. This gives the ill-conditioned matrix R. This problem will effect the calculation of θ in (2.48). For f, $\bar{f}$ and h filters in (2.48), we have used the same model order but in real there are not. These shortcomings in the method have also been highlighted by others during the project.

4 Result

4.1 Introduction

In this Chapter, different simulation and measurement results have been presented. The results of two-tone complex signal, with equal amplitude and equal phase shift used to obtain the spectrally pure signal. Both the conventional polynomial $\phi_m(\cdot)$ and orthogonal polynomial $\psi_m(\cdot)$ have been used to generate the signals. The device under test was IQ modulation mismatch and amplifier deficiencies in the signal generator. The least squares method was used for system identification and design of the digital predistorter.
For the measurements performed in this work, the signals have been generated using the vector signal generator and the measurements are performed using the spectrum analyzer. Synchronization has been used to find the delay between two signals. Synchronization is a definition of cross-correlation between input and output signal and phase shift, with reference to Section 2.7.3.

4.2 Simulation results

In this Section, a two-tone complex signal has been generated. A two-tone signal was at frequencies 34.53 MHz and 45.16 MHz with equal amplitude at 6.9 dBm and equal phase shift. A tow-tone signal without predistortion has the mirror distortion at frequencies -34.53 MHz and -45.16 MHz, with equal amplitude at -73.0 dBm. The tow-tone signal with predistortion have the mirror distortion at frequencies -34.53 MHz and -45.16 MHz, with amplitude -86.3 dBm and -85.6 dBm, respectively. With reference to Figure 4.1-4.2 the mirror distortion have been reduced after predistortion design. The mirror distortion have been reduced 13.3 dBm at frequency -34.53 MHz and 12.6 dBm at frequency -45.16 MHz. we could reduce mirror distortion by using γ, but we have not used it. Because γ is a small speech, then all columns in $\bar{S}$ will be small compared to the columns of S matrix. This gives the ill-conditioned matrix R. This problem will effect

the calculation of θ in (2.48). So we haven't used γ in the $\bar{S}$ matrix. The intermodulation products for two-tone signal for $\phi_m(\cdot)$ function without predistortion were at frequency 23.91 MHz with amplitude -59.0 dBm and at frequency 55.78 MHz with amplitude -59.0 dBm. The intermodulation products for two-tone signal for $\phi_m(\cdot)$ function with predistortion were at frequency 23.91 MHz with amplitude -97.1 dBm and at frequency 55.78 MHz with amplitude -96.4 dBm (see Figures 4.3-4.4). The intermodulation products for two-tone signal for $\psi_m(\cdot)$ function without predistortion were at frequency 23.91 MHz with amplitude -59.0 dBm and at frequency 55.78 MHz with amplitude -59.0 dBm. The intermodulation products for two-tone signal for $\psi_m(\cdot)$ function with predistortion were at frequency 23.91 MHz with amplitude -93.6 dBm and at frequency 55.78 MHz with amplitude -94.9 dBm (see Figures 4.5-4.6).

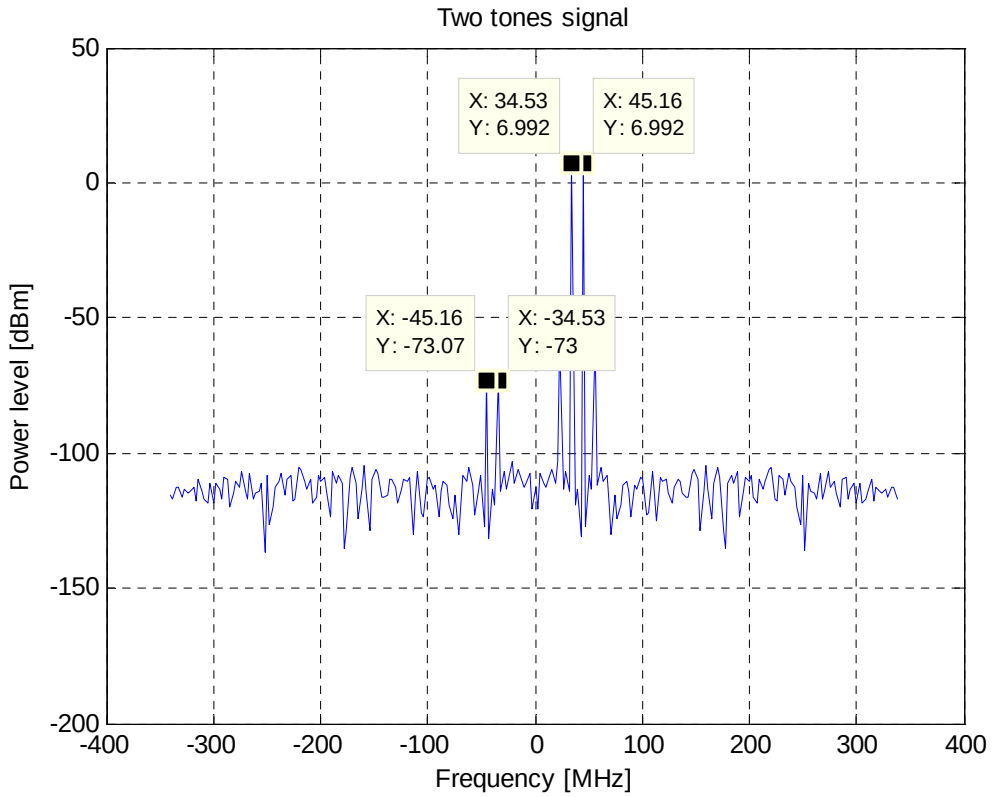

Figure 4.1. Power spectrum of two-tone signal without predistortion

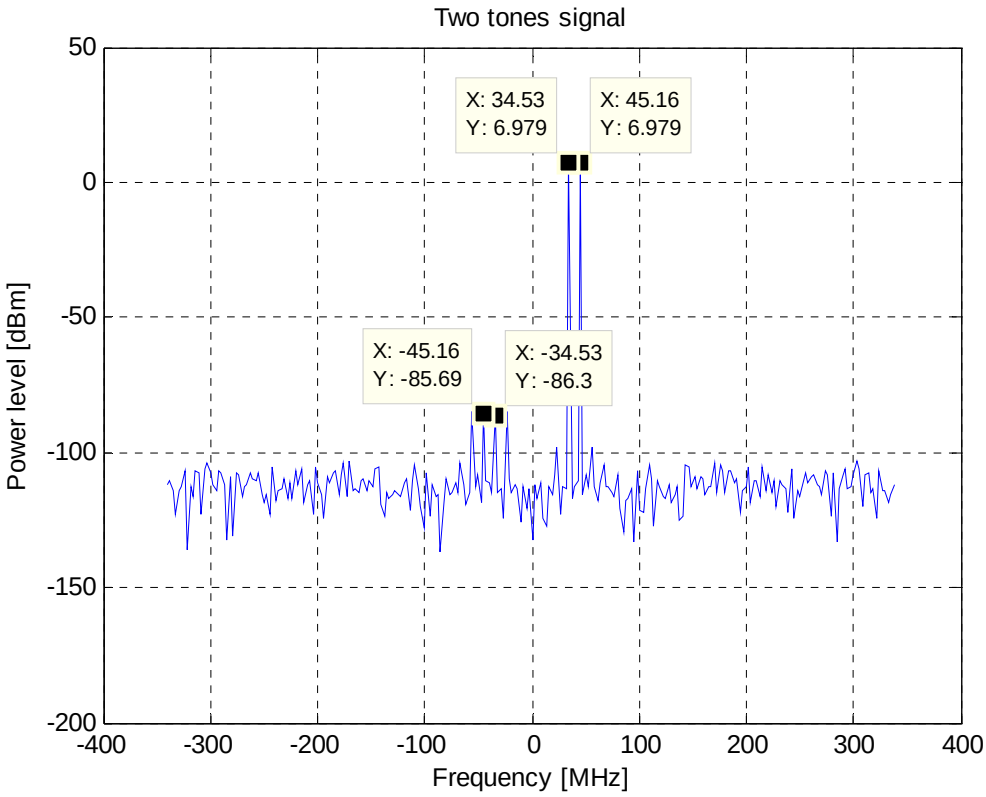

Figure 4.2. Power spectrum of two-tone signal with predistortion

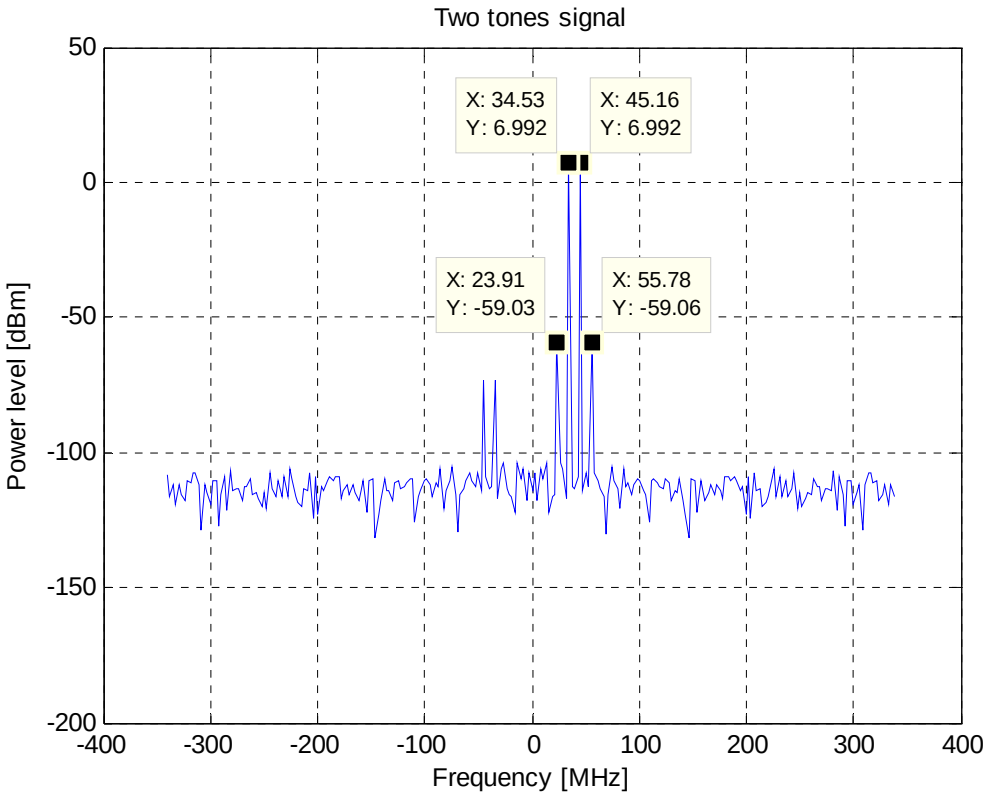

Figure 4.3. Power spectrum of two-tone signal for $\phi_m(\cdot)$ function without predistortion

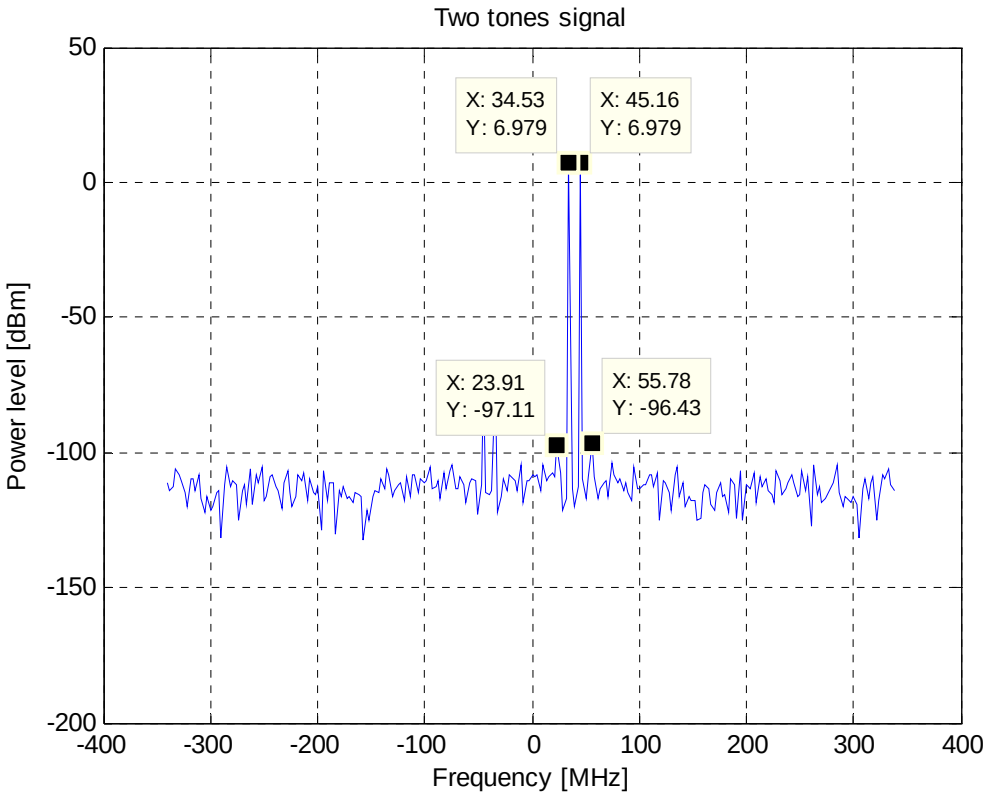

Figure 4.4. Power spectrum of two-tone signal for $\phi_m(\cdot)$ function with predistortion

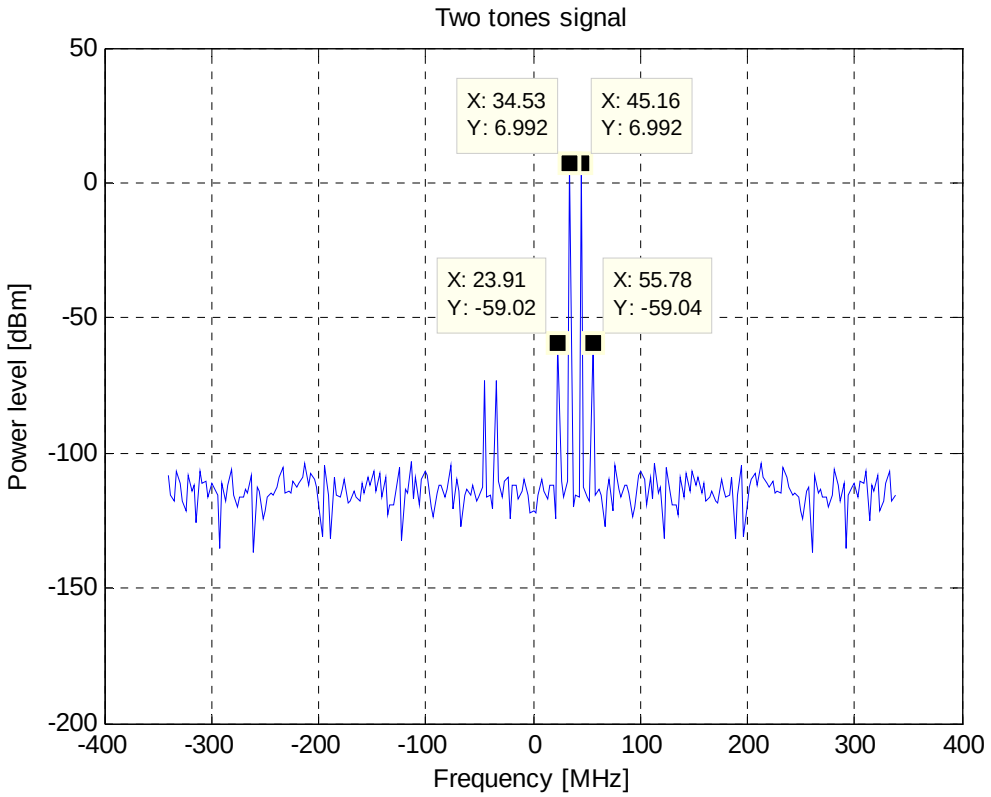

Figure 4.5. Power spectrum of two-tone signal for $\psi_m(\cdot)$ function without predistortion

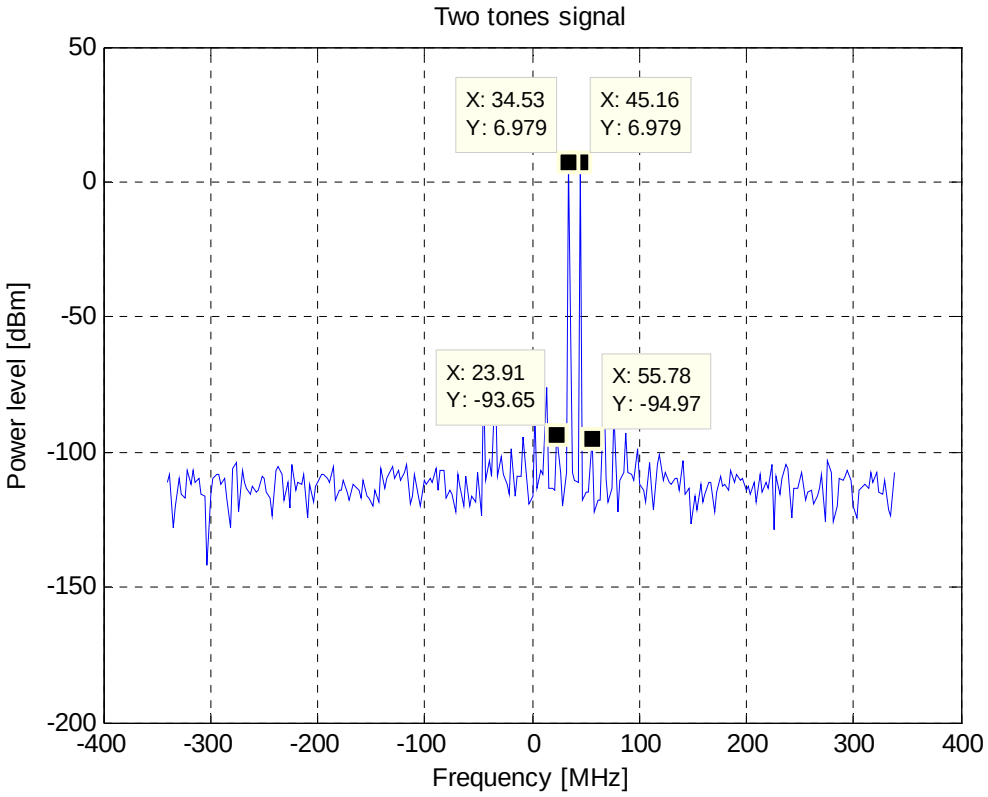

Figure 4.6. Power spectrum of two-tone signal for $\psi_m(\cdot)$ function with predistortion

4.3 Measurement results

The signal used for this measurement was a two-tone complex signal that is generated by personal computer software and sent to the vector signal generator. The measurement was performed using the spectrum analyzer. In the SA the center frequency of the signal was 2.14 GHz and a bandwidth of 20 MHz. The resolution bandwidth is an important parameter in the configuration of the spectrum analyzer was set to 10 KHz, in order to achieve high enough signal to noise ratio without falling in to long sweep time. The measurement was done at a sampling frequency of 80 MHz.

A two-tone complex signal has been generated. A two-tone signal was at frequencies 3.012 MHz and 8.088 MHz with equal amplitude at 6.2 dBm and equal phase shift. The intermodulation products for two-tone signal for $\phi_m(\cdot)$ function without predistortion were at frequency -2.065 MHz with amplitude -51.0 dBm and at frequency 13.16 MHz with amplitude -55.2 dBm. The intermodulation products for two-tone signal for $\phi_m(\cdot)$ function with predistortion were at frequency -2.065 MHz with amplitude -58.0 dBm and at frequency 13.16 MHz with amplitude -71.3 dBm (see Figures 4.7-4.8). The intermodulation products for two-tone signal for $\psi_m(\cdot)$ function without predistortion were at frequency -2.065 MHz with amplitude -50.8 dBm and at frequency 13.16 MHz with amplitude -55.1 dBm. The intermodulation products for two-tone signal for $\psi_m(\cdot)$ function with predistortion were at frequency -2.065 MHz with amplitude -59.8 dBm and at frequency 13.16 MHz with amplitude -88.6 dBm (see Figures 4.9-4.10).

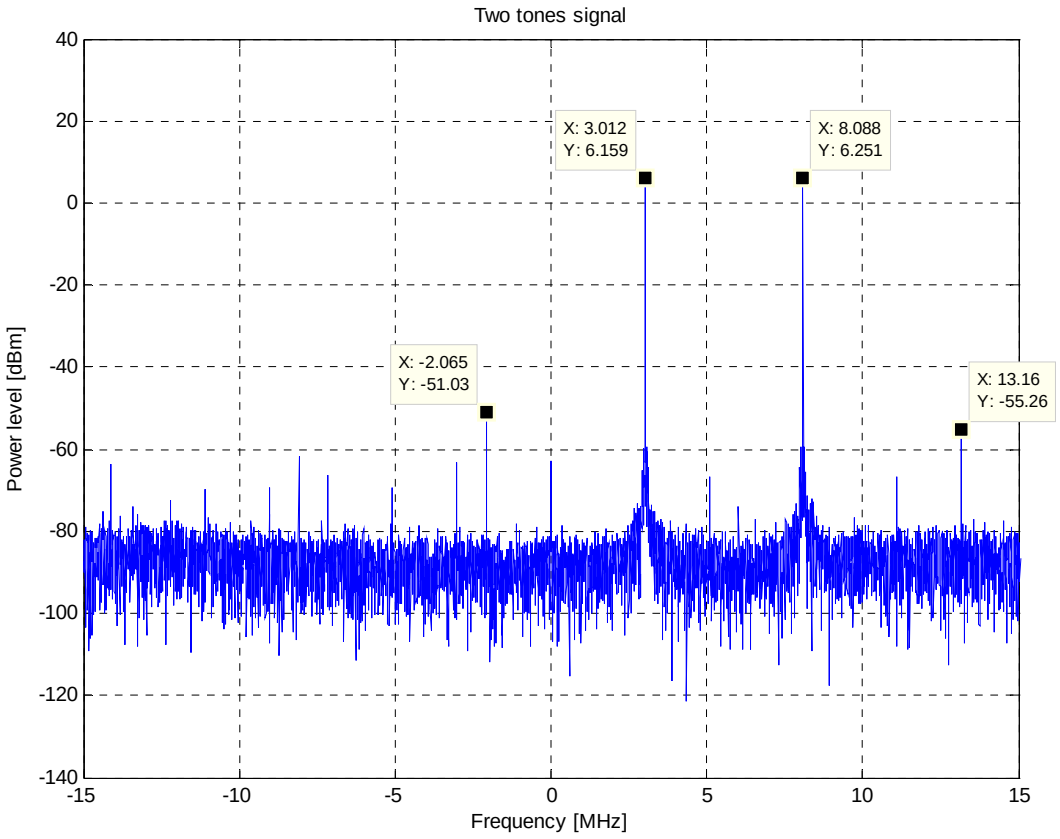

Figure 4.7. Power spectrum of two-tone signal for $\phi_m(\cdot)$ function without predistortion

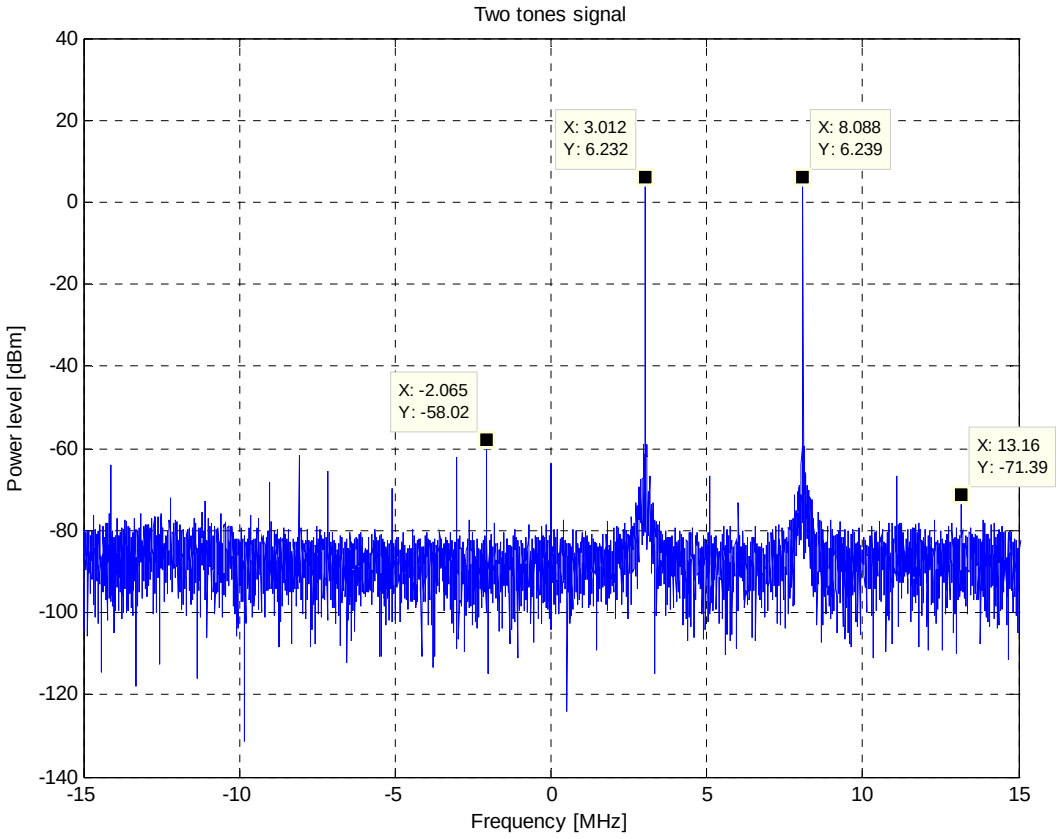

Figure 4.8. Power spectrum of two-tone signal for $\phi_m(\cdot)$ function with predistortion

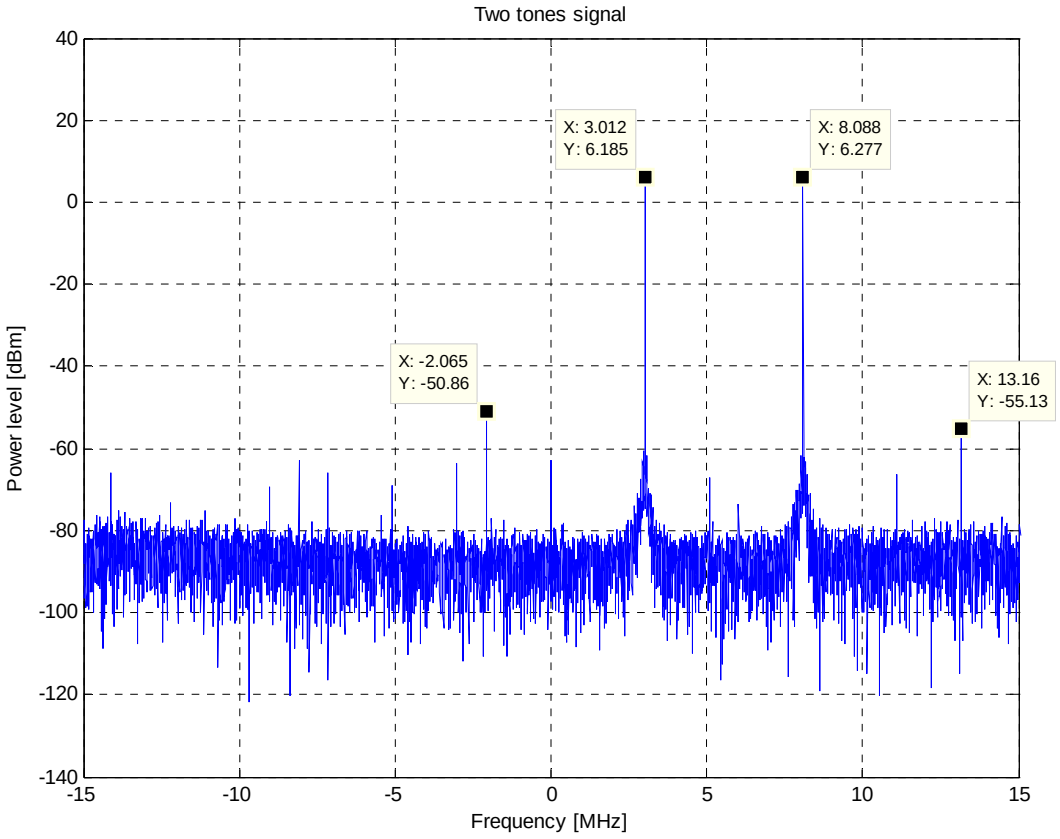

Figure 4.9. Power spectrum of two-tone signal for $\psi_m(\cdot)$ function without predistortion

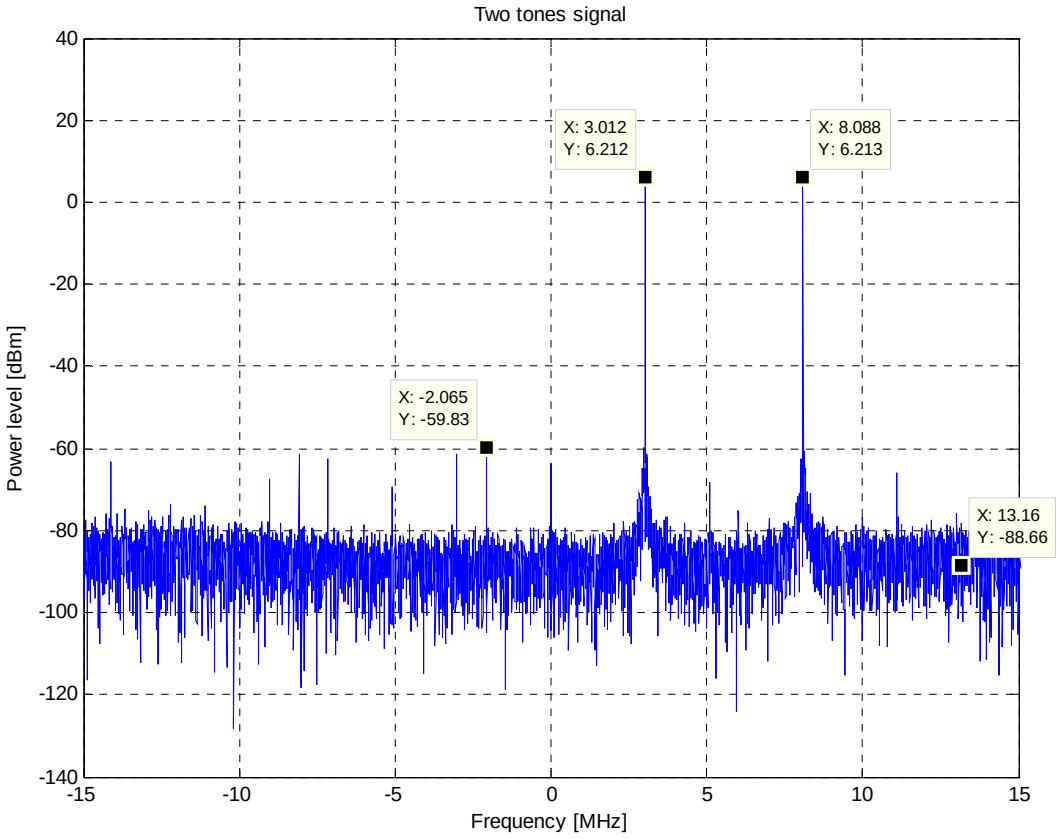

Figure 4.10. Power spectrum of two-tone signal for $\psi_m(\cdot)$ function with predistortion

5 Discussion

In this project, the problems I have encountered were that the matrix R is ill-conditioned and the reason of that was the column of the matrix $\bar{S}$ has low values because we calculate $\bar{S}$ matrix with γ. Since γ is a small speech, then all columns in $\bar{S}$ will be small compared to the columns of S matrix. This gives the ill-conditioned matrix R. For f, $\bar{f}$ and h filters we have used the same model order but in real there are not. These shortcomings in the method have also been highlighted by others during the project.

We have studied parallel project, [19] there they have achieved a good result by using a novel predistorter structure for the joint mitigation of power amplifier and IQ modulator impairments in wideband direct-conversion radio transmitters. The predistorter was based on the parallel Hammerstein or memory polynomial predistorter, yielding a predistorter which is completely linear in the parameters. In the estimation stage the indirect learning architecture is utilized. The proposed technique is the first technique to consider the joint estimation and mitigation of frequency-dependent PA and modulator impairments. It is a similar solution, but do not have the same disadvantages.

In [19], the PA predistorter is a parallel Hammerstein or memory polynomial predistorter with the static nonlinearities given by the orthogonal polynomials, the IQ predistorter is of the general two-filter type where one filter $G_1(z)$, is filtering the original or non-conjugate signal, and the other, $G_2(z)$, is filtering the conjugated signal and LO leakage compensator. The filters of the PA PD and IQ PD are in cascade, making their separate estimation difficult. A joint power amplifier and IQ modulator predistorter was suitable for mitigating frequency dependent impairments. The PD is completly linear in the parameters thus allowing easy estimation of PD parameters with linear least-squares. The simulation and measurement analysis show good performance.

6 Conclusion

A simulation system and a measurement system have been designed in a data program (Matlab) and a parsimoniously parameterized digital predistorter design used to generate a spectrally pure signal. The objective of this project was to implement and evaluate the theory parts using data program (Matlab). The parallel Hammerstein structure has been used that is consist of the nonlinearity followed by a linear filter and it is useful for digital predistortion of power amplifier. In this work, two polynomial model have been used in power amplifier modelling and predistorter design. the conventional polynomial $\phi_m(\cdot)$ and orthogonal polynomial $\psi_m(\cdot)$ have been used to generate signals.

The simulation results for two-tone signal presented in Section 4.2, the plots showed that the intermodulation products have been reduced after predistortion design. The intermodulation products for $\phi_m(\cdot)$ function at frequency 23.91 MHz have been reduced 38.0 dBm and at frequency 55.78 MHz have decreased 37.3 dBm. The intermodulation products for $\psi_m(\cdot)$ function at frequency 23.91 MHz have decreased 34.6 dBm and at frequency 55.78 MHz have decrased 35.9 dBm. The measurement results for two-tone signal presented in Section 4.3, the plots showed that the intermodulation products have been reduced after predistortion design. The intermodulation products for $\phi_m(\cdot)$ function at frequency -2.065 MHz have decreased 6.9 dBm and at frequency 13.16 MHz have decreased 16.1 dBm. The intermodulation products for $\psi_m(\cdot)$ function at frequency -2.065 MHz have decreased 8.9 dBm and at frequency 13.16 MHz have decreased 33.5 dBm. The results showed that the $\psi_m(\cdot)$ function generally yield better power amplifier modeling accuracy as well as predistortion linearization performance then the $\phi_m(\cdot)$ function.

We did not achieve the performance increase that we wish or hope we have identify possible causes of it and also studied alternative solutions, unfortunately, we have not had the opportunity in this project to implement and verify these theories.

7 References

[1] P. Händel, "Dynamic nonlinear pre-distortion of signal generators for improved dynamic range", Draft for a journal paper, Oct. 2008.

[2] C. Luque and N. Björsell, "Improved dynamic range for multi-tone signal using model-based pre-distortion," *13 Th Workshop on ADC Modeling and Testing*, florence, Italy, 2008, September 22-24.

[3] N. Björsell," Modeling Analog to Digital converters at Radio Frequency". Doctoral thesis in Telecommunications, KTH School of Electrical Engineering, Stockholm, 2007.

[4] M. Valkama, "Advanced I/Q signal processing for wideband receivers: models and algorithms, PhD thesis, Tampere University of Technology, November, 2001.

[5] G. Yang, G. Vos and H. Cho**. "**I/Q modulator image rejection through modulation pre- distortion**",** *IEEE Vehicular Technology Conference*, 1996**.**

[6] M. Isaksson," Behavioral Modeling of Radio Frequency Power Amplifiers ". doctoral Thesis in Telecommunications, KTH School of Electrical Engineering, Stockholm, 2007.

[7] C. Luque," Model-based pre-distortion for signal generators", Department of technology, vol. Master thesis. Gävle: University of Gävle, 2007.

[8] M. Isaksson, D. Wisell and D. Rönnow, "Wide-Band Dynamic Modeling of Power amplifiers Using Radial-Basis Function Neural Neworks", Microwave Theory and Techniques, Volume 53, Issue 11, Nov. 2005.

[9] N. Ceylan, "Linearization of power amplifiers by means of digital predistortion," in *Technische Fakultät*, vol. Doctor-Ingenier. Erlangen: Universität Erlangen-Nurnberg, 2005.

[10] E. Aschbacher, "Digital Pre-distortion of Microwave Power Amplifiers", doctoral thesis, university of technology, wien, 2005.

[11] G. Xing, M. Shen, and H. Liu, "Frequency Offset and I/Q Imbalance Compensation for Direct-Conversion Receivers", *IEEE transaction on Wireless Communication*, Mars 2005.

[12] L. Anttila, M. Valkama and M. Renfors, ”Frequency selective I/Q mismatch calibration of wideband direct-conversion transmitters”, *IEEE Transactions on Circuits and Systems* – II: *Express briefs*, Vol. 55, No. 4 April 2008, pp. 359-363.

[13] D. Rönnow and M. Isaksson, ”Digital predistortion of radio frequency power amplifiers using Kautz-Volterra model”, Vol. 42, issue 13, pp. 780-782, University of Gävle, June 2006. .

[14] P.L. Landin, M. Isaksson and P .Händel, “On accurate power amplifier behavioural models,” *IEEE Transactions on Microwave theory and techniques, submitted*, April 2008.

[15] R. Raich, H. Qian and T. Zhou, “Orthogonal polynomials for power amplifier modelling and predistorter design”, *IEEE Transactions on Vehicular Technology*, Vol. 53, No. 5, Septembe2004,pp.1468-1479.

[16] D. Wisell, “A Baseband Time Domain Measurement System for Dynamic characterization of Power Amplifiers with High Dynamic Range over Large bandwidth”. Instrumentation and Measurement Technology Conference, 2003.

[17] J. Proakis, Digital Communications: McGraw-Hill, 1995.

[18] Rhode & Schwarz FSQ 26 Operating Manual.

[19] L. Anttila, M. Valkama, P. Händel, “Joint Mitigation of Power Amplifier and Modulator Impairments in Wideband Direct-Conversion Transmitters”, Draft for a journal paper, April. 2009.